ELECTRON TRANSPORT INSIDE NANOPOROUS ZNO-BASED DYE-SENSITIZED SOLAR CELL

H. Abdullah[1*], A. Omar[1], N. P. Ariyanto[1], S. Shaari[1]

[1] *Department of Electrical, Electronic and Systems Engineering, Faculty of Engineering & Built Environment, Universiti Kebangsaan Malaysia, 43600 Bangi, Selangor, Malaysia*
**huda@eng.ukm.my*

Keywords: dye-sensitized solar cell, electrons, impedance, ZnO

Abstract

Electron diffusion, recombination and transportation inside nanoporous ZnO-based dye-sensitized solar cell play an important role in photovoltaic efficiency and stability. In this research work, electrochemical impedance spectroscopic is used to investigate the ionic mechanisms inside the cell. An appropriate equivalent circuit model has also been modelled to interpret the impedance spectra and frequency response of the circuit. Three impedance spectra regions provide further information of the electrons kinetics and energy of the solar cell. The cell parameters such as the electron lifetime, τ_{eff} of 6.36 ms was measured as much shorter than TiO_2-based DSSC (25 - 160 ms), effective electron diffusion coefficient, D_{eff} of 4.7e-^{7} cm^2s^{-1} and effective rate constant for recombination k_{eff} of 157 s^{-1} have been analyzed accordingly. The highest overall power conversion efficiency was up to 2.45 %. The results and analysis proved the previous work on the nanotechnology fabrication of the dye-sensitized solar cell.

1 Introduction

Dye-sensitized solar cell (DSSC) has received great interest in solar technology research and development which is easy to manufacture, low cost technique and high chances for large-scale production [1-3]. Inside the DSSC structures, the injected electrons are injected either from the photoexcited dye molecules adsorbed in the metal oxide surface or from the transparent conducting oxide (TCO) substrate [4]. For the substrate-injected electrons, the concentrations will decrease due to the electron transfer across the oxide/electrolyte interface where the electron flux, J_n is zero. Furthermore, this kind of electron transportation produces either low or high recombination. For low recombination, the electron diffusion length (L_n) is much larger than the film thickness (L). In the other case, the electron concentration decreases rapidly near the injection boundary. The mechanism of the injected electrons or back reaction with redox species inside the DSSC can further be investigated by using various techniques such as transient photocurrent or photovoltage measurements, intensity-modulated photocurrent/photovoltage spectroscopy (IMPS/IMVS) or open-circuit decay technique. However, in photoelectrochemical applications, other technique performs much better analysis named as electrochemical impedance spectroscopy (EIS). EIS is a steady-state approach by measuring a current response and small ac voltage as a function of frequency. This kind of approach applies small ac perturbation on the whole cell [5-6]. Bisquert and Kern

et al have derived an impedance equation based on two different impedance models to elucidate in details the electron diffusion and recombination in TiO_2 thin film layer [5, 7-8].

Currently, TiO_2-based DSSC has achieved 11 % power conversion efficiency at AM 1.5 [9]. Although it provides large surface area for dye adsorption, slow electron transport has limited their efficiency [10]. Consequently, ZnO which have similar band gap and conduction band energies to TiO_2 (3.37 eV) [2] have received great interests to study about electron kinetics inside it. Hence, electron diffusion, recombination and transportation are the command terms being named to differentiate the kinetic processes. The equivalent circuit model or the impedance model of the cell usually represented as a transmission line model with appropriate resistance and capacitance values. Different models have been proposed to obtain a relevant spectrum models such as anomalous diffusion processes, multiple trapping and non-uniform conductivity and capacitance [4]. Meanwhile, Paasch (2000) mentioned that the existence of current generator in the equivalent circuit model influenced the diffusion impedances [11].

In the present paper, analysis of the electron transport inside the nanoporous ZnO-based DSSC are explained accordingly which is an extension to the work done by Ariyanto (2010) [12]. Meanwhile, the solar cells were prepared as explained in our previous published reports [13-15].

2 Experimental Details

2.1 Fabrication of dye-sensitized solar cell

In summary, a chemical bath deposition method was used to prepare the precursor solution of 0.05 M zinc nitrate hexahydrate and 1 M urea. In a closed beaker, fluorine-doped tin oxide (FTO)-coated glass substrate (sheet resistance ~10 Ω/cm^2) was immersed into the solutions and heated in oven at different temperature, 60 °C and 80 °C for 24 hours deposition time. After deposition, the films were rinsed in distilled water and dried. The films were treated by calcination at 300 °C in air for 30 minutes. A photoanode was prepared by immersing the ZnO thin film into 0.5 mM ethanolic N719 dye solutions for 30 minutes and rinsed in absolute ethanol (99.9 %). Counter electrode was prepared by depositing a platinum paste onto the FTO substrate by using a screen printing technique. The deposition was followed by a drying process at 110 °C and annealing at 450 °C for one hour which produce a quasi transparent counter electrode. Iodolyte MPN 100 (Solaronix SA) was used as an electrolyte.

2.2 EIS measurement

Current density - voltage (*J-V*) characteristic was recorded using Keithley 237 Source Measure Unit under 1000 W/m^2 illumination of 1.5 AM simulated sunlight. The measurement was conducted within an active area of 0.25 cm^2. Electrochemical impedance spectroscopy (EIS) was performed by using GAMRY Series G300 potentiostat. The spectrums were recorded under 1000 W/m^2 illumination of OSRAM Halogen 50 W with UV filter. Open-circuit voltage (V_{oc}) and 10 mV AC signal were applied under frequency range of 10 mHz - 100 kHz.

3 Results and discussion

3.1 Photovoltaic performance

Any kind of solar cells performances are measured from the I-V or J-V characteristics consist of short-circuit current density, open-circuit voltage, fill-factor and power conversion efficiency. Table 1 summarized the photovoltaic performance of two nanoporous ZnO-based DSSCs named as sample A and B. The performances of the solar cells were influenced by the deposition temperature of the chemical bath solution since sample A was deposited at 60 °C and sample B at 80 °C, accordingly.

Sample	Deposition temperature [°C]	J_{sc} [mA cm^{-2}]	V_{oc} [V]	*FF*	η [%]
A	60	6.732	0.533	0.505	1.81
B	80	8.752	0.557	0.503	2.45

Table 1. Properties determined by electrochemical impedance spectroscopy.

From the results, higher deposition temperature and longer deposition time (24 hours) have increased the short-circuit current density (J_{sc}) from 6.732 mA cm^{-2} to 8.752 mA cm^{-2}. Thus, higher dye adsorption also occurred for better electron transport and diffusion from the dye to the semiconductor layer of nanoporous ZnO. The internal process of the electron kinetics can be analyzed in details by using EIS units.

3.2 Transmission line model of DSSC

EIS is an advanced technique to analyze the internal mechanisms inside ZnO- or TiO_2-based DSSCs especially in terms of the electron transport and charge recombination inside the cells. A transmission line model or equivalent circuit model was implemented in the EIS analysis to fit the impedance spectra of the DSSC. Analysis is carried out for two samples; photoanode A and B which have been immersed at 60 °C and 80 °C for 24 hours, respectively. Figure 1 shows a suitable transmission line model of the nanoporous ZnO-based DSSC [16].

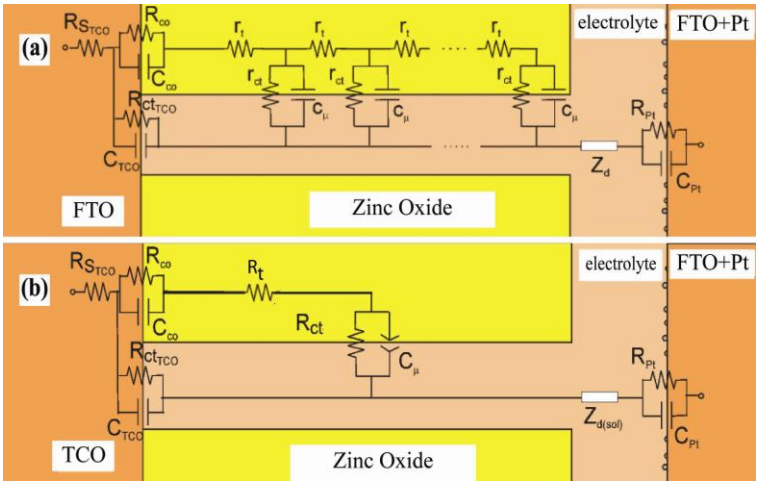

Figure 1. (a) Transmission line model of DSSC (b) Simplified circuit of DSSC [16].

R_S represents sheet resistance of the conducting substrate, R_{CO} and C_{CO} represent resistance and capacitance at the semiconductor interface with conducting substrate, R_{TCO} and C_{TCO} represent charge-transfer resistance and double-layer capacitance of exposed conducting substrate toward electrolyte, r_{ct} represents charge transfer resistance of electron in semiconductor porous film under recombination process towards electrolyte, c_μ represents chemical capacitance in semiconductor porous film, r_t represents transport resistance of nanoparticle in porous film, Z_d represents Warburg impedance element of diffusion of redox species in electrolyte, R_{Pt} and C_{Pt} represent charge-transfer resistance and double-layer capacitance on counter electrode [5, 16-17].

The model corresponds to the following impedance equation:

$$Z = \left(\frac{R_t R_{ct}}{1+\frac{i\omega}{\omega_{ct}}}\right)^{1/2} coth\left[\left(\frac{\omega_{ct}}{\omega_t}\right)^{1/2}\left(1+\frac{i\omega}{\omega_{ct}}\right)^{1/2}\right] \quad (1)$$

where R_t is the diffusion resistance, R_{ct} is the recombination resistance, ω_{ct} is the rate constant for recombination, ω is the angular frequency and $i = \sqrt{-1}$ [4, 7, 15, 17]. Equation 1 is valid for a homogeneous element of the circuit model not considering the current generator effect [5]. Furthermore, ω_{ct} is also known as angular frequency of the electron recombination equivalent to the effective rate constant for recombination of the electron (k_{eff}) and electron lifetime ($\tau_{eff} = 1/k_{eff}$) [18]. Meanwhile, ω_t is the charge transfer constant or characteristic frequency of diffusion in a finite layer ($\omega_t = D_{eff}/L^2 = 1/R_t C_\mu$), D_{eff} is the effective electron chemical diffusion coefficient and L is the film thickness of the photoanode. This equation is valid for homogeneous and inhomogeneous distribution of electrons inside the semiconductor layer [17].

Figure 2 illustrates the impedance spectra obtained for two DSSCs; sample A and B. The spectrums were fitted by using the above equivalent circuit model. Three typical arcs or ideal spectrum of DSSC were identified from the samples; high frequency arc due to charge transfer at the counter electrode (1 kHz - 100 kHz), intermediate or middle frequency arc (1 Hz - 1 KHz) attributes to electron transport in nanostructure ZnO thin film and low frequency arc reflects to ionic diffusion in the electrolyte layer [6-7].

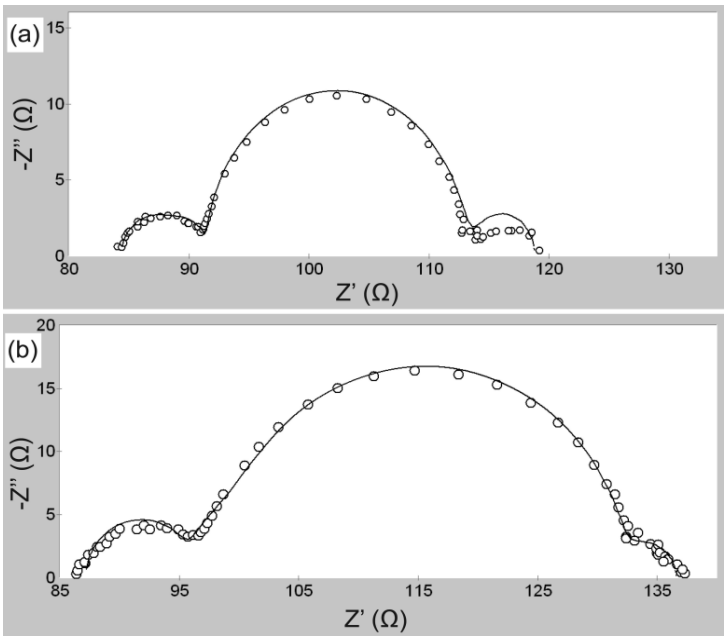

Figure 2. (a) Spectrum of electrochemical impedance spectroscopy (o) and fitting curve (-) of DSSC with photoanode deposited at (a) 60 °C and (b) 80 °C for 24 hours [12].

Both samples have peak position of middle frequency peak at 25 Hz (or f_{max} = 25 Hz), given as:

$$\omega_{max} = k_{eff} = \frac{1}{\tau_{eff}} \quad (2)$$

or

$$\omega_{max} = \omega_{ct} = k_{eff} \quad (3)$$

Electron lifetime inside the porous photoanode can be calculated by using Eq. 4. Effective electron diffusion coefficient (D_{eff}) and effective electron diffusion length (L_n) can be calculated accordingly by using Eq. 5 and Eq. 6 [5, 12, 15].

$$\tau_{eff} = \frac{1}{\omega_{ct}} = \frac{1}{2\pi f_{max}} \tag{4}$$

$$D_{eff} = \frac{R_{ct}}{R_t}\frac{L^2}{\tau_{eff}} \tag{5}$$

$$L_n = L\sqrt{\frac{R_{ct}}{R_t}} \tag{6}$$

Sample	L [µm]	R_{ct} [Ω.cm^2]	R_t [Ω.cm^2]	τ_{eff} [ms]	k_{eff} [s^{-1}]	D_{eff} [cm^2.s^{-1}]	L_n [µm]
A	18	3.794	1.135	6.36	157	1.7 x 10^{-3}	32.9
B	24	3.216	0.683	6.36	157	4.2 x 10^{-3}	52.1

Table 2. Properties determined by electrochemical impedance spectroscopy.

Table 2 shows the properties derived from EIS spectrum analysis. Both samples have short electron lifetime (τ_{eff} = 6.36 ms) which is much shorter than TiO_2-based DSSC but higher effective electron diffusion coefficient compared to TiO_2-based DSSC which has about 10^{-7} to 10^{-4} cm^2.s^{-1}. Short electron lifetime of ZnO indicates faster and aggressive recombination between the injected electron in the semiconductor and electrolyte layers [3, 6-7, 18-21]. In the case of nanoporous ZnO prepared at longer deposition time with higher surface area and porosity has also increased the dye adsorption and the same time improved the electron transfer rate inside samples A and B.

Moreover, the spectrums also correspond to transport resistance (R_t) and charge-transfer resistance (R_{ct}) [22]. From Table 2, R_t are less than R_{ct} ($R_t < R_{ct}$) indicates that low recombination occurs inside the DSSC. In addition, low recombination also increase the overall power conversion efficiency of sample B up to 2.45 % compared to sample A (1.81 %). R_t and R_{ct} also signifies a normalized value of diffusion length which should be greater than 1 [20]:

$$\frac{L_t}{L} = \sqrt{\frac{R_{ct}}{R_t}} \tag{7}$$

From the obtained values of R_t and R_{ct}, both values are greater than 1.

3.2 Impedance analysis inside electrolyte

Electrochemical impedance spectroscopy unit can be used to investigate the impedance inside the electrolyte for example Warburg impedance. It was analyzed as an impedance inside the electrolyte at low frequency region. The ionic diffusion of tri-iodide ($I_{I_3^-}$) ions has higher molarities compared to iodide (I^-) ions. The Warburg impedance is defined as:

$$Z_d = \frac{Z_0}{\sqrt{j\omega}} \tanh\left(\frac{d_{I_3^-}}{\sqrt{D_{I_3^-}}}\sqrt{j\omega}\right) \quad (8)$$

and

$$Z_0 = \frac{RT}{n^2F^2c_0A\sqrt{D_{I_3^-}}} \quad (9)$$

where Z_d represents Warburg impedance inside the liquid electrolyte, Z_0 represents limited Warburg parameter, $D_{I_3^-}$ represents tri-iodide diffusion coefficient ion, $d_{I_3^-}$ represents triiodide diffusion distance ion or film thickness between photoanode and counter electrode, ω represents measured angular frequency, R represents gas molarities constant, T represents absolute temperature (T = 300 K), n represents amount of diffused electrons for each redox reactions (n = 2), F represents Faraday constant, c_0 represents total molarities of triiodide ions and A represents electrode surface area.

Fitting of the impedance spectrums were conducted by using Gamry Echem Analyst v.5.06 software. The Warburg parameter and diffusion constant were defined as in Eq. 10 and 11:

$$Y_0 = \frac{1}{Z_0} \quad (10)$$

where Y_0 is Warburg parameter and Z_0 is limited Warburg parameter, with:

$$B = \frac{d_{I_3^-}}{\sqrt{D_{I_3^-}}} \quad (11)$$

B is the diffusion time constant, $D_{I_3^-}$ represents tri-iodide diffusion coefficient ion, $d_{I_3^-}$ represents triiodide diffusion distance ion or film thickness between photoanode and counter electrode. $D_{I_3^-}$ is defined as:

$$D_{I_3^-} = \left(\frac{L_{electrolyte}}{B}\right)^2 \quad (12)$$

Parafilm M with a thickness around 100 µm has been used to support the electrolyte inside the ZnO-based DSSC. Sample A with 18 µm photoanode thicknesses covered almost 82 µm electrolyte thicknesses. However, for sample B the electrolyte thickness reduced to 76 µm.

Sample	***L*** **[µm]**	$L_{electrolyte}$ **[µm]**	Y_{Od} **[S. s$^{1/2}$. cm^{-2}]**	***B*** **[s$^{1/2}$]**	$D_{I_3^-}$ **[cm^2. s^{-1}]**
A	18	82	0.215	1.091	5.6 x 10^{-5}
B	24	76	0.283	1.769	1.8 x 10^{-5}

Table 3. Properties determined by electrochemical impedance spectroscopy.

From the obtained values as in Table 3, electrolyte of sample A contains 5.6 x 10^{-5} $cm^2.s^{-1}$ tri-iodide ion which is greater than sample B. However, due to homogeneity effect and spectra analysis of sample B ($D_{I_3^-}$ = 1.8 x 10^{-5} $cm^2.s^{-1}$), this value is defined as analogous to the results measured by Anneke et al (2001) [23].

Conclusion

EIS is an effective tool to investigate about electron transport, diffusion and recombination properties inside the nanoporous ZnO-based DSSC. A few terms have been calculated based on the equivalent circuit model and impedance spectra fitting. Short electron lifetime, τ_{eff} shows faster recombination occurred between the injected electron and oxidized electrolyte. Effective electron diffusion coefficient, D_{eff} also found as much lower than TiO_2-based DSSC. Electron lifetime and electron diffusion coefficient determined the electron diffusion length, L_n which depends on the amount of light illuminated on the photoanode. Large value of L_n compare to the film thicknesses, L ($L_n > L$) identified low recombination effects inside the sample B which also gained higher efficiency (η = 2.45 %).

Acknowledgement

This work has been supported by (Project No.: UKM-DLP-2011-056) and Photonics Technology Laboratory, Department of Electrical, Electronic & Systems Engineering, Faculty of Engineering & Built Environment, Universiti Kebangsaan Malaysia, 43600 UKM Bangi, Selangor, Malaysia.

References

[1] Juan B., David C., Gary H., Sven R., Arie Z. Physical chemical principles of photovoltaic conversion with nanoparticulate, mesoporous dye-sensitized solar cells. *J. Phys. Chem. B,* **108**, pp. 8106-8118 (2004).

[2] Qifeng Z., Christopher S. D., Xiaoyuan Z., Guozhong C., ZnO nanostructures for dye-sensitized solar cells. *Advanced Material* **21**, pp. 4087-4108 (2009).

[3] Wei-Hao C., Chia-Hua L., Hsin-Ming C., Hsiu-Fen L., Shih-Chieh L., Jenn-Ming W., Wen-Feng H., Efficient electron transport in tetrapod-like ZnO metal-free dye-sensitized solar cells, *Energy & Env. Sci.*, **2**, pp. 694-698 (2009).

[4] Ángeles P., Germà G.-B., Iván M.-S., Juan B. Electrochemical impedance spectra for the complete equivalent circuit of diffusion and reaction under steady-state recombination current. *Phys. Chem. Chem. Phys.*, **6**, pp. 2983-2988 (2004).

[5] Juan B. Theory of the impedance of electron diffusion and recombination in a thin layer. *J. Phys. Chem. B,* **106**, pp. 325-333 (2002).

[6] Qian W., Jacques-E. M., Michael G. Electrochemical impedance spectroscopic analysis of dye-sensitized solar cells. *J. Phys. Chem. B*, **109**, pp. 14945-14953 (2005).

[7] Motonari A., Masaru S., Jinting J., Yukio O., Seiji I., Determination of parameters of electron transport in dye-sensitized solar cells using electrochemical impedance spectroscopy, *J. of Phys. Chem. B*, **110**, pp. 13872-13880 (2006).

[8] Kern R., Sastrawan R., Ferber J., Stangl R., Luther J., Modeling and interpretation of electrical impedance spectra of dye solar cells operated under open-circuit conditions, *Electrochem. Acta* **47**, pp. 4213-4225 (2002).

[9] Michael G., Conversion of sunlight to electric power by nanocrystalline dye-sensitized solar cells, *J. of Photochem. and Photobiol. A: Chem.* **164**, pp. 145-153 (2003).

[10] Chen-Hao K., Jih-Jen W., Chemical bath deposition of ZnO nanowire-nanoparticle composite electrodes for use in dye-sensitized solar cells, *Nanotechnology* **18**, pp. 1-9 (2007).

[11] Paasch G., The transmission line equivalent circuit model in solid-state electrochemistry, *Electrochemistry Comm.* **2**, pp. 371-375 (2000).
[12] Nugroho P. A., *Study on synthesis of mesoporous zinc oxide film as photoanode towards performance of dye-sensitized solar cell*, Master's Thesis, Univ. Kebangsaan Malaysia, (2011).
[13] Huda A., Nugroho P. A., Huda A., Sahbuddin S., Brian Y., Junaidi S., Study of porous nanoflake ZnO for dye-sensitized solar cell application, *American J. of Eng. and Applied Scien., 2*, pp. 236-240 (2009).
[14] Nugroho P. A., Huda A., Sahbuddin S, Junaidi S., Brian Y., Preparation and characterisation of porous nanosheets zinc oxide films: based on chemical bath deposition, *World Applied Sci. J.*, **6**, pp. 764-768 (2009).
[15] Nugroho P. A., Huda A., Junaidi S., Brian Y., Sahbuddin S., Fabrication of zinc oxide-based dye-sensitized solar cell by chemical bath deposition, *Func. Mat. Letters.*, **4**, pp. 303-307 (2010).
[16] Qian W., Seigo I., Michael G., Francisco F.-S., Iván M.-S., Juan B., Takeru B., Hachiro I., Characteristics of high efficiency dye-sensitized solar cells, *J. Phys. Chem. B,* **110**, pp. 25210-25221 (2006).
[17] Francisco F.-S., Juan B., Germà G.-B., Gerrit B., Anders H., Influence of electrolyte in transport and recombination in dye-sensitized solar cells studied by impedance spectroscopy. *Sol. Energy Mat. & Sol. Cells*, **87**, pp. 117-131 (2005).
[18] Hsin-Ming C., Wei-Hao C., Chia-Hua L., Song-Yeu T., Wen-Feng H., Formation of branched ZnO nanowires from solvothermal method and dye-sensitized solar cells applications, *J. of Phys. Chem.*, **112**, pp. 16359-16364 (2008).
[19] María Q., Tomas E., Anders H., Gerrit B., Comparison of dye-sensitized ZnO and TiO_2 solar cells: studies of charge transport and carrier lifetime. *J. of Physical Chemistry C*, **111**, pp. 1035 – 1041 (2007).
[20] Francisco F.-S., Juan B., Emilio P., Luis O., Daibin K., Shaik M. Z., Michael G., Correlation between photovoltaic performance and impedance spectroscopy of dye-sensitized solar cells based on ionic liquids. *J. of Phys. Chem. C*, **111,** pp. 6550 – 6560 (2007).
[21] Alex B. F. M., Márcio S. G., Francisco F.-S., Juan B., Michael J. P., Joseph T. H., Electron transport in dye-sensitized solar cells based on ZnO nanotubes: evidence for highly efficient charge collection and exceptionally rapid dynamics, *J. of Phys. Chem.*, **113,** pp. 4015-4021 (2009).
[22] Lu-Yin L., Min-Hsin Y., Chuan-Pei L., Chen-Yu C., R. V., Kuo-Chuan H., Enhanced performance of a flexible dye-sensitized solar cell with a composite semiconductor film of ZnO nanorods and ZnO nanoparticles, *Electrochimica Acta*, **62**, pp. 341-347 (2012).
[23] Anneke H., Andreas G., Diffusion in the electrolyte and charge-transfer reaction at the platinum electrode in dye-sensitized solar cells, *Electrochimica Acta*, **46**, pp. 3457-3466 (2001).